

# Application of *Butea monosperma* (Palasha) Leaves Extract as Green Corrosion Inhibitor for Mild Steel in Hydrochloric Acid Solution: A Theoretical and Electrochemical Approach

Ambrish Singh<sup>1</sup>, M. A. Quraishi<sup>2,\*</sup>, Eno E. Ebenso<sup>3</sup>

<sup>1</sup> Department of Chemistry, Faculty of Technology and Sciences, Lovely Professional University, Phagwara, Punjab-144411 (India)

<sup>2</sup> Department of Applied Chemistry, Institute of Technology, Banaras Hindu University, Varanasi 221 005 (India)

<sup>3</sup> Department of Chemistry, School of Mathematical & Physical Sciences, North-West University (Mafikeng Campus), Private Bag X2046, Mmabatho 2735, South Africa

\*E-mail: [maquraishi@rediffmail.com](mailto:maquraishi@rediffmail.com)

Received: 17 October 2012 / Accepted: 14 November 2012 / Published: 1 December 2012

---

The inhibition effect of Palasha (*Butea monosperma*) leaves extract on mild steel in 1M HCl was investigated using gravimetric, potentiodynamic polarization and electrochemical impedance spectroscopy. Potentiodynamic polarization results revealed that the studied extract is a mixed-type inhibitor. The inhibition efficiency increased up to 96% at 300 ppm. The  $R_{ct}$  of inhibited system increased and double layer capacitance  $C_{dl}$  decreased with increasing inhibitor concentration. UV-Visible spectroscopic investigation of inhibited system suggested a complexation between the active molecules of extract and the metal surface atoms. Quantum chemical calculations supported the adsorption of inhibitor molecules onto the metal surface.

---

**Keywords:** Mild steel; EIS; Acid corrosion; Quantum calculations; UV-Visible Spectroscopy

## 1. INTRODUCTION

Acid solutions are mostly used in the industries for removal of rusts and scales. Use of inhibitors is one of the common methods in industries for protection of metallic corrosion in acid solutions. The known hazardous effect of most synthetic corrosion inhibitors has motivated scientists to use natural products as corrosion inhibitors. These are inexpensive, readily available and renewable feedstocks, environmentally friendly and ecologically acceptable materials.

Generally, the compounds containing  $\pi$ -bonds and heteroatoms (N, S or O) exhibits good inhibitive properties. Several works on plant extracts as green corrosion inhibitors have been reported

in literature [1-11]. Palasha leaves are used in cuisines of various cultures around the world, as a whole and grounded form. It helps to add an earthy and warming feeling to cooking; making it a staple in certain stews and soups, as well as curries and chilies [12, 13]. The main phytoconstituent of Palasha leaves is Butrin (Figure 1), which is likely to impart good corrosion inhibition activity due to presence of aromatic ring and heteroatoms in its molecular structure. Survey of literature reveals that no work has been reported on Palasha extract as corrosion inhibitor.

The gravimetric and electrochemical techniques were used to study the effect of leaf extract on mild steel in 1M HCl. Several isotherms were tested for their relevance to describe the adsorption behavior of the compounds studied. The effect of temperature on the corrosion behavior of steel in the absence and presence of the leaves extract was also studied.

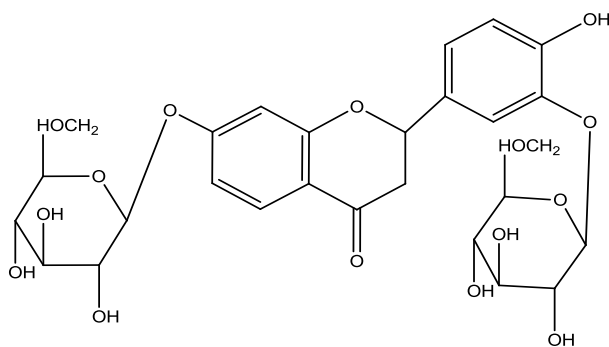


**Figure 1.** Structure of Butrin

## 2. EXPERIMENTAL

### 2.1 Inhibitor

For stock solution, the dried Palasha (*Butea monosperma*) leaves were powdered (10 g) and further soaked in double distilled water (500 mL) and refluxed for 5 h. The aqueous solution was filtered and concentrated to 100 mL. This extract was used to study the corrosion inhibition properties. Corrosion tests were performed on a mild steel of the following percentage composition: Fe 99.30%, C 0.076%, Si 0.026%, Mn 0.192%, P 0.012%, Cr 0.050%, Ni 0.050%, Al 0.023%, and Cu 0.135%. Prior to all measurements, the mild steel specimens were abraded successively with silicon carbide papers from 600 to 1200 grades. The specimens were washed thoroughly with double distilled water, degreased with acetone and finally dried in hot air blower. And then, the specimens were placed in the desiccator for backup. The test solution of 1 M HCl was prepared by dilution of analytical grade HCl (37%) with double distilled water and all experiments were carried out in unstirred solutions. The rectangular specimens with dimension  $2.5 \times 2.0 \times 0.025 \text{ cm}^3$  were used for weight loss experiments and of size  $1.0 \times 1.0 \text{ cm}^2$  (exposed) with a 7.5 cm long stem (isolated with commercially available lacquer) were used for electrochemical measurements.

## 2.2. Weight loss method

Weight loss measurements were performed on rectangular mild steel samples having size  $2.5 \times 2.0 \times 0.025 \text{ cm}^3$  by immersing the mild steel coupons into acid solution (100 mL) in absence and presence of different concentrations of Palasha (*Butea monosperma*) leaves extract. After the elapsed time, the specimen were taken out, washed, dried and weighed accurately. All the tests were conducted in aerated 1 M HCl. The inhibition efficiency ( $\eta$  %) and surface coverage ( $\theta$ ) were determined by using following equation;

$$\theta = \frac{w_o - w_i}{w_o} \quad (1)$$

$$\eta\% = \frac{w_o - w_i}{w_o} \times 100 \quad (2)$$

where  $w_i$  and  $w_o$  are the weight loss values in presence and absence of inhibitor, respectively.

The corrosion rate ( $C_R$ ) of mild steel was calculated using the relation:

$$C_R (\text{mmy}^{-1}) = \frac{87.6 \times w}{AtD} \quad (3)$$

where  $w$  is weight loss of mild steel (mg),  $A$  the area of the coupon ( $\text{cm}^2$ ),  $t$  is the exposure time (h) and  $D$  the density of mild steel ( $\text{g cm}^{-3}$ ) [14].

## 2.3 Electrochemical impedance spectroscopy

The EIS tests were performed at 308 K in a three electrode assembly. A saturated calomel electrode was used as the reference; a  $1 \text{ cm}^2$  platinum foil was used as counter electrode. All potentials are reported versus SCE. Electrochemical impedance spectroscopy measurements (EIS) were performed using a Gamry instrument Potentiostat/Galvanostat with a Gamry framework system based on ESA 400 in a frequency range of  $10^{-2}$  Hz to  $10^5$  Hz under potentiodynamic conditions, with amplitude of 10 mV peak-to-peak, using AC signal at  $E_{\text{corr}}$ . Gamry applications include software DC105 for corrosion and EIS300 for EIS measurements, and Echem Analyst version 5.50 software packages for data fitting. The experiments were carried out after 30 min. of immersion in the testing solution

The inhibition efficiency of the inhibitor was calculated from the charge transfer resistance values using the following equation:

$$\mu\% = \frac{R_{\text{ct}}^i - R_{\text{ct}}^0}{R_{\text{ct}}^i} \times 100 \quad (4)$$

where,  $R_{ct}^0$  and  $R_{ct}^i$  are the charge transfer resistance in absence and in presence of inhibitor, respectively.

#### 2.4 Potentiodynamic polarization

The electrochemical behavior of mild steel sample in inhibited and uninhibited solution was studied by recording anodic and cathodic potentiodynamic polarization curves. Measurements were performed in the 1 M HCl solution containing different concentrations of the tested inhibitor by changing the electrode potential automatically from -250 to +250 mV versus corrosion potential at a scan rate of 1 mV s<sup>-1</sup>. The linear Tafel segments of anodic and cathodic curves were extrapolated to corrosion potential to obtain corrosion current densities ( $i_{corr}$ ). From the polarization curves obtained, the corrosion current ( $i_{corr}$ ) was calculated by curve fitting using the equation:

$$I = i_{corr} \left[ \exp\left(\frac{2.3\Delta E}{b_a}\right) - \exp\left(-\frac{2.3\Delta E}{b_c}\right) \right] \quad (5)$$

The inhibition efficiency was evaluated from the measured  $i_{corr}$  values using the relationship:

$$\mu\% = \frac{i_{corr}^0 - i_{corr}^i}{i_{corr}^0} \times 100 \quad (6)$$

where,  $i_{corr}^0$  and  $i_{corr}^i$  are the corrosion current density in absence and presence of inhibitor, respectively.

#### 2.5 Linear polarization measurement

The corrosion behavior was studied with polarization resistance measurements ( $R_p$ ) in 1 M HCl solution with and without different concentrations of studied inhibitor. The linear polarization study was carried out from cathodic potential of -20 mV versus OCP to an anodic potential of + 20 mV versus OCP at a scan rate 0.125 mV s<sup>-1</sup> to study the polarization resistance ( $R_p$ ) and the polarization resistance was evaluated from the slope of curve in the vicinity of corrosion potential. From the evaluated polarization resistance value, the inhibition efficiency was calculated using the relationship:

$$\mu\% = \frac{R_p^i - R_p^0}{R_p^i} \times 100 \quad (7)$$

where,  $R_p^0$  and  $R_p^i$  are the polarization resistance in absence and presence of inhibitor, respectively.

2.6. UV-Visible spectroscopy

UV-Visible absorption spectra were measured with Hitachi U-2900 double beam spectrophotometer. The Palasha (*Butea monosperma*) leaves extract solution (300 ppm) and the washing solution obtained after 5 hrs of mild steel immersion at 308 K were subjected to UV-Visible absorption detection.

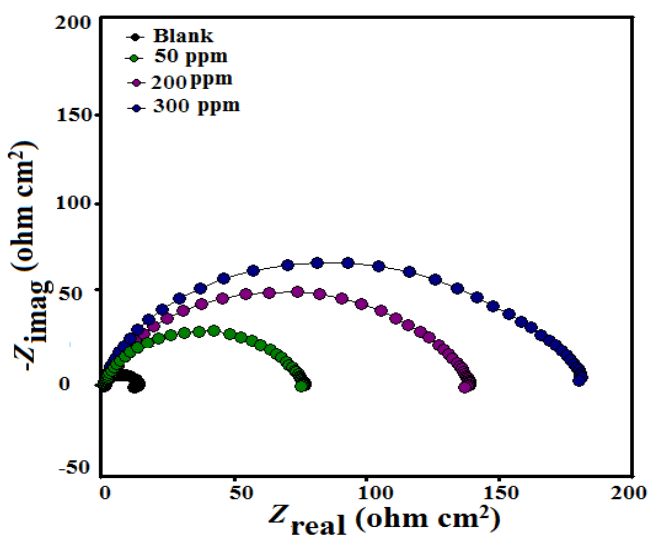
2.7. Theoretical study

All the calculations were performed with Gaussian 03 for windows. The molecular structures of the neutral species were fully and geometrically optimized using the functional hybrid B3LYP (Becke, three-parameter, Lee-Yang-Parr exchange-correlation function) Density function theory (DFT) formalism with electron basis set 6-31G (\*, \*) for all atoms. The quantum chemical parameters obtained were EHOMO, ELUMO, EHOMO-LUMO ( $\Delta E$ ),  $\mu$ , total energy and Mulliken charge on heteroatoms (O).

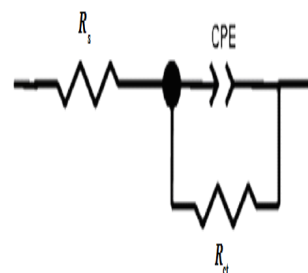
3. RESULTS AND DISCUSSION

3.1 Electrochemical impedance spectroscopy

Impedance spectra for mild steel in 1 M HCl in absence and presence of different concentrations of leaves extract are shown in the form of Nyquist plots (Fig. 2a), Bode-modulus plots (Fig. 2d) and Phase angle plots (Fig. 2e). It followed from Fig. 2a that the impedance of the inhibited mild steel increases with increase in the inhibitor concentration and consequently the inhibition efficiency also increases.



(a)



(b)

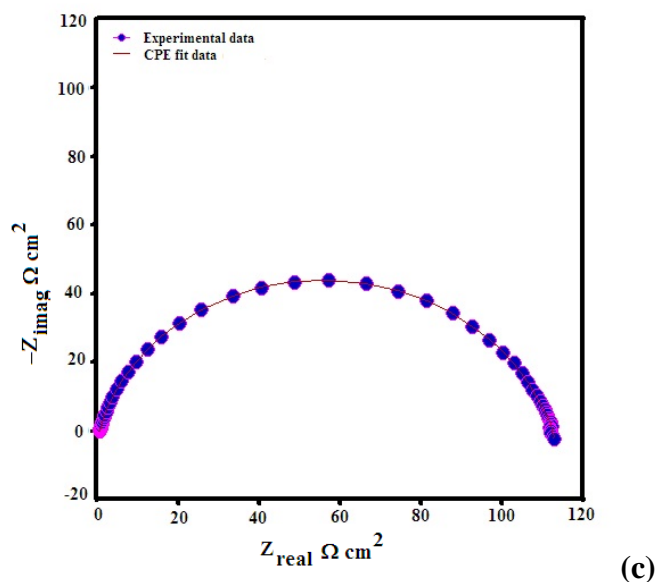


**Figure 2.** (a) Nyquist plots of mild steel in 1 M HCl in absence and presence of different concentrations of Palasha (*Butea monosperma*) leaves extract (b) equivalent circuit used to fit the impedance data (c) Nyquist plot with CPE fit data

A depressed semicircle is mostly referred to as frequency dispersion which could be attributed to different physical phenomena such as roughness and inhomogeneities of the solid surfaces, impurities, grain boundaries and distribution of the surface active sites [15]. The fact that this semicircle cannot be observed after the addition of higher concentration supports our view [16, 17]. Different corrosion parameters derived from EIS measurements are presented as Table 1. It is shown from Table 1 that  $R_{ct}$  of inhibited system increased from  $78 \Omega\text{cm}^2$  to  $182 \Omega\text{cm}^2$  and double layer capacitance  $C_{dl}$  decreased from  $42 \mu\text{Fcm}^{-2}$  to  $18 \mu\text{Fcm}^{-2}$  with increasing inhibitor concentration. This decrease in  $C_{dl}$  results from a decrease in local dielectric constant and/or an increase in the thickness of the double layer, suggested that inhibitor molecules inhibit the iron corrosion by adsorption at the metal/acid interface.

To get more accurate fit of these experimental data, the measured impedance data were analyzed by fitting in to equivalent circuit given in Fig. 2b. Excellent fit with this model was obtained for all experimental data.

Mathematically, amplitude of CPE is given by the relation:

$$Z_{\text{CPE}} = Q^{-1}(j\omega)^{-n} \quad (8)$$

where  $Q$  is the magnitude of the CPE,  $j$  is the imaginary unit,  $\omega$  is the angular frequency ( $\omega = 2\pi f$ , the frequency in Hz), and  $n$  is the phase shift which gives details about the degree of surface inhomogeneity. When  $n = 1$ , this is the same equation as that for the impedance of a capacitor, where  $Q = C_{dl}$ . In fact, when  $n$  is close to 1, the CPE resembles a capacitor, but the phase angle is not  $90^\circ$ . It

is constant and somewhat less than  $90^\circ$  at all frequencies thereby suggesting the deviation from idealized capacitive behavior.

The electrochemical parameters are listed in Table 1.  $C_{dl}$  values derived from CPE parameters are listed in Table 1. For providing simple comparison between the capacitive behaviors of different corrosion systems, the values of  $Q$  were converted to  $C_{dl}$  using the relation [18]:

$$C_{dl} = Q(\omega_{max})^{n-1} \quad (9)$$

where,  $\omega_{max}$  represents the frequency at which the imaginary component reaches a maximum. It is the frequency at which the real part ( $Z_r$ ) is midway between the low and high frequency x-axis intercepts.

**Table 1.** Calculated electrochemical parameters for mild steel in absence and presence of different concentrations of Palasha (*Butea monosperma*) leaves extract

Inhibitor concentration(ppm)	$R_{ct}$ ( $\Omega \text{ cm}^2$ )	$n$	$Y_0$ ( $10^{-6} \Omega^{-1} \text{ cm}^{-2}$ )	$C_{dl}$ ( $\mu\text{F cm}^{-2}$ )	$\eta\%$
Blank	8	0.847	250	69	-
50	78	0.846	98	42	89
200	145	0.849	67	25	94
300	182	0.852	49	18	96

### 3.2 Potentiodynamic Polarization

The Tafel polarization curves of mild steel in hydrochloric acid solution, in the absence and presence of different concentrations of Palasha (*Butea monosperma*) leaves extract, are presented in Fig. 3 and listed in Table 2. The maximum inhibition efficiency (95%) was obtained at a concentration of 300 ppm.

Addition of the Palasha (*Butea monosperma*) leaves extract to acid media affected both the cathodic and anodic parts of the curves. For the inhibited system, if the displacement in  $E_{corr}$  value is greater than 85 mV relative to uninhibited system than the inhibitor is classified as cathodic or anodic type. In our case, the maximum displacement of  $E_{corr}$  value is 43 mV, hence the Palasha (*Butea monosperma*) leaves extract is classified as a mixed-type inhibitor. From the polarization curves it was noted that the curves were shifted toward lower current density region and  $\beta_c$  and  $\beta_a$  values did not showed any significant change [19, 20]. The inhibition efficiency values in the Table 2 showed that the Palasha (*Butea monosperma*) leaves extract acted as very effective corrosion inhibitor for mild steel in HCl solution and its capacity of inhibition increased with increase of concentration.

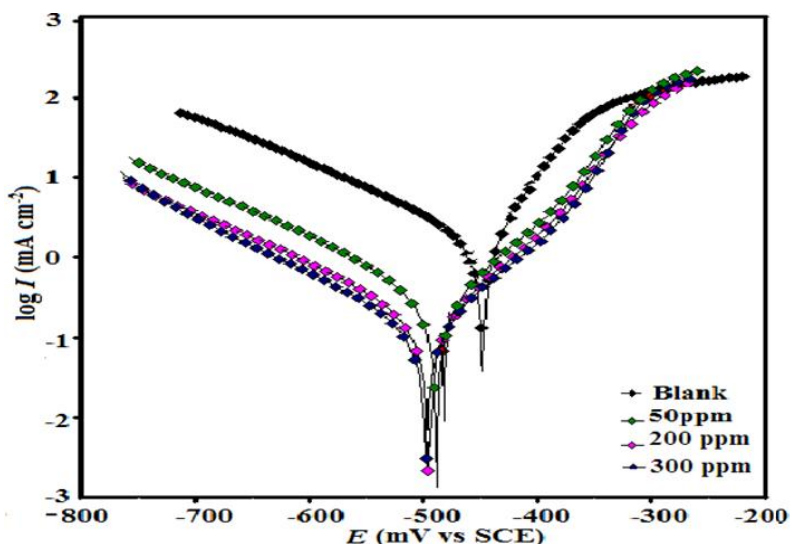


**Figure 3.** Tafel polarization curves for corrosion of mild steel in 1 M HCl in the absence and presence of different concentrations of Palasha(*Butea monosperma*) leaves extract

**Table 2.** Polarization data for MS in 1 M HCl in absence and presence of different concentration of Palasha(*Butea monosperma*) leaves extract

Inhibitor concentration(ppm)	Tafel Polarization			Linear Polarization			
	$E_{corr}$ (mV vs SCE)	$\beta_a$ (mV/dec)	$\beta_c$ (mV/dec)	$I_{corr}$ ( $\mu A cm^2$ )	$\eta\%$	$R_p$ ( $\Omega cm^2$ )	$\eta\%$
Blank	-446	90	121	1540	-	8	-
50	-483	89	143	325	78	79	89
75	-483	97	197	175	88	151	94
100	-489	110	209	74	95	189	95

### 3.3 Linear polarization measurement

The inhibition efficiencies obtained from polarization resistance are presented in Table 2. The linear polarization values increased from 79  $\Omega cm^2$  to 189  $\Omega cm^2$  resulting in a high inhibition efficiency of 95% at 300 ppm. The results obtained from Tafel polarization and EIS showed good agreement with the results obtained from linear polarization resistance.

### 3.4 Weight loss measurements

#### 3.4.1 Effect of inhibitor concentration

The effect of inhibitor concentration on inhibition efficiency of steel in 1 M HCl was examined thoroughly. Maximum inhibition efficiency obtained was 94% at 300 ppm in HCl solution. The values

of percentage inhibition efficiency ( $\eta\%$ ) and corrosion rate ( $C_R$ ) obtained from weight loss method at different concentrations of Palasha (*Butea monosperma*) leaf extract at 308 K are summarized in Table 3.

**Table 3.** Corrosion rate and Inhibition efficiency values for the corrosion of mild steel in aqueous solution of 1 M HCl in the absence and in the presence of different concentrations of Palasha (*Butea monosperma*) leaves extract from weight loss measurements at 308 K

Name of Inhibitor	Conc. of Inhibitor (ppm)	Surface Coverage ( $\theta$ )	$\eta\%$	$C_R$ (mmy <sup>-1</sup> )
1 M HCl	-	-	-	77
Palasha( <i>Butea monosperma</i> ) leaves extract	50	0.40	40	45
	200	0.75	75	19
	300	0.94	94	5

### 3.5. UV-Visible Spectroscopy

UV-Visible spectroscopy provides a strong evidence for the formation of a metal complex [21]. We obtained UV-Visible absorption spectra for optimum concentration of Palasha (*Butea monosperma*) leaves extract at 308 K before and after 5 hours immersion of mild steel specimen. The electronic absorption spectrum of Palasha (*Butea monosperma*) leaves extract before the mild steel immersion shows two bands in UV-region as shown in Figure 4. These bands may arise due to  $\pi$ - $\pi^*$  and n-  $\pi^*$  transitions with a considerable charge transfer character. After 5 hrs immersion of mild steel change in the position of absorption maximum or change in the values of absorbance indicate the formation of a complex between two species in solution. However, there was no any significant change in the shape of the spectra.

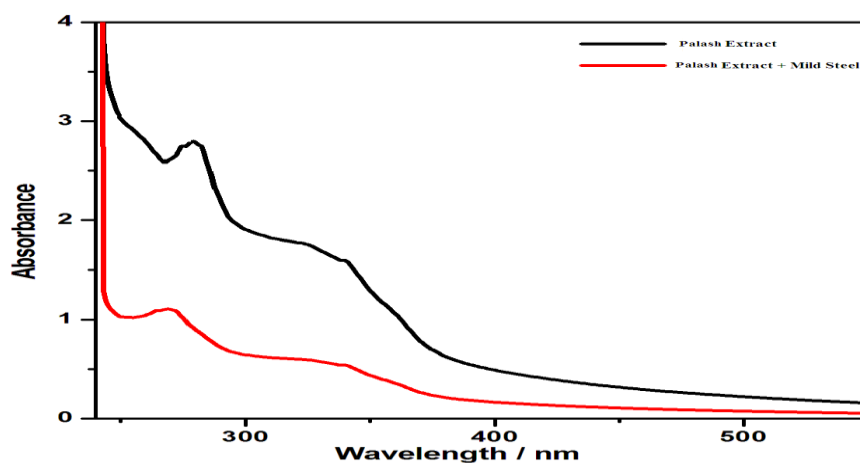


**Figure 4.** UV-Visible spectroscopy with Palasha extract before and after 5 hours immersion of mild steel

These experimental findings provide strong evidence for the complex formed between  $\text{Fe}^{2+}$  and Palasha (*Butea monosperma*) leaves extract in 1 M HCl solution. UV-Visible observation confirms the formation of protective film of inhibitor on metal surface.

### 3.6. Quantum Chemical Calculations

Quantum chemical calculations were carried out in order to investigate adsorption and inhibition mechanism of studied inhibitor molecules [22]. Figure 5 shows full geometry optimization of the inhibitor molecules with Mulliken charges.

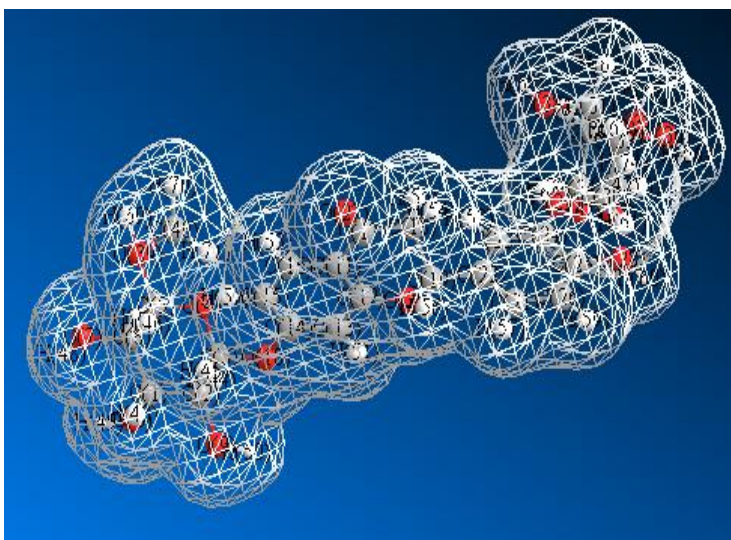


**Figure 5.** Optimized molecular structure with Mulliken charges of the active constituent (Butrin) of Palasha (*Butea monosperma*) leaves extract

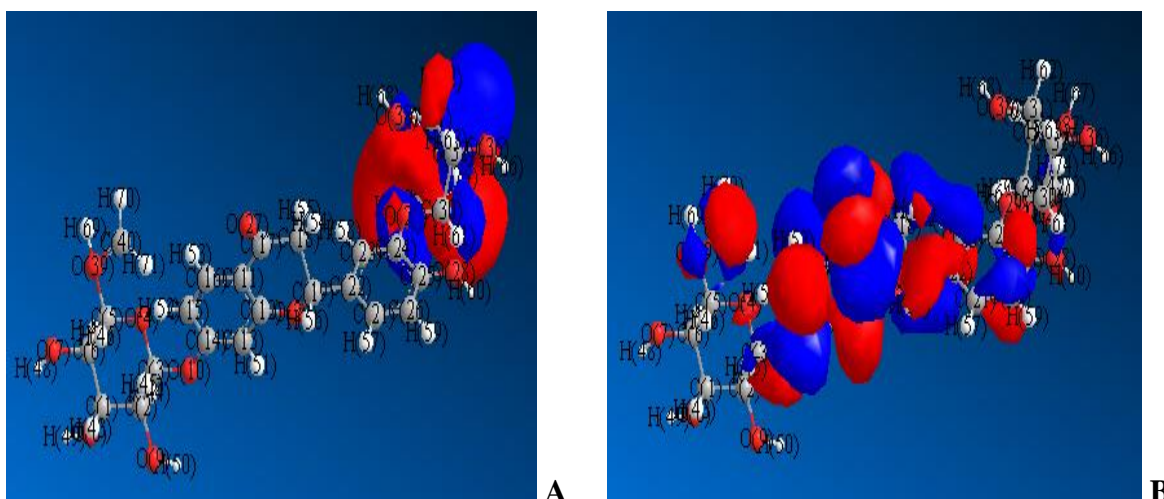


**Figure 6.** The frontier molecular orbital density distribution of the active constituent (Butrin) of Palasha (*Butea monosperma*) leaves extract (a) HOMO (b) LUMO)

The Frontier molecular orbital (FMO) density distributions of Butrin present in Palasha (*Butea monosperma*) leaves extract are shown in Figure 6 (a-b). In order to construct a composite index of an inhibitor molecule it may be important to focus on parameters that directly influence the electronic interaction of the inhibitor molecules with the metal surface. These are mainly:  $E_{\text{HOMO}}$ ,  $E_{\text{LUMO}}$ ,  $\Delta E$  ( $E_{\text{LUMO}}-E_{\text{HOMO}}$ ), and dipole moment  $\mu$ . The values of calculated quantum chemical parameters such as  $E_{\text{HOMO}}$ ,  $E_{\text{LUMO}}$ ,  $\Delta E$  ( $E_{\text{LUMO}}-E_{\text{HOMO}}$ ), and  $\mu$  of Butrin are listed in Table 4.

Frontier orbital theory is useful in predicting adsorption centers of the inhibitor molecules responsible for the interaction with surface metal atoms.

Terms involving the frontier molecular orbitals could provide fruitful contribution, because of the inverse dependence of stabilization energy on orbital energy difference. Lower the value of  $E_{\text{LUMO}}$ , the more probable; it is that the molecule would accept electrons [23]. As for the values of  $\Delta E$  ( $E_{\text{LUMO}}-E_{\text{HOMO}}$ ) concern; lower values of the energy difference  $\Delta E$  will cause higher inhibition efficiency because the energy to remove an electron from the last occupied orbital will be low. For the dipole moment ( $\mu$ ), higher values of  $\mu$  will favor accumulation of the inhibitor in the surface layer [24, 25].

**Table 4.** Calculated Quantum chemical parameters of studied inhibitor

Quantum Parameters	Butrin
HOMO (hartree)	-0.4368
LUMO (hartree)	0.0809
$\Delta E_{\text{LUMO-HOMO}}$ (hartree)	0.5177
Dipole Moment ( $\mu$ )	5.1442

#### 4. MECHANISM OF INHIBITION

Adsorption of active constituent from extract arises from the donor acceptor interactions between free electron pairs of hetero atoms and  $\pi$ -electrons of multiple bonds, vacant d-orbitals of Fe. In case of adsorption of organic compounds on the metallic surface, planarity of molecules must also be taken in to consideration.

The protonated Butrin from Palasha (*Butea monosperma*) leaves extract may adsorb on surface through synergistic effect with  $\text{Cl}^-$  in hydrochloric acid solution [26]. It is well known fact that the inhibitors which not only offer electrons to metal atoms but also have unoccupied higher energy orbitals to accept electrons from d-orbital of metal atom for strengthening of bonding interaction [27, 28]. It is not possible to consider a single adsorption mode between inhibitor and metal surface because of the complex nature of adsorption and inhibition of a given inhibitor. It is well known that the steel surface bears positive charge in acid solution; it is difficult for the protonated molecules to approach the positively charged mild steel surface ( $\text{H}_3\text{O}^+$ /metal interface) due to the electrostatic repulsion. Since chloride ions have a smaller degree of hydration, they could bring excess negative charges in the

vicinity of the interface and favor more adsorption of the positively charged inhibitor molecules, the protonated inhibitors adsorb through electrostatic interactions between the positively charged molecules and the negatively charged  $\text{Cl}^-$  ions. Thus, there is a synergism between adsorbed  $\text{Cl}^-$  ions and protonated inhibitors. Hence, we can assume that inhibition of mild steel corrosion in 1 M HCl is due to the adsorption of extract constituents on the mild steel surface.

## 5. CONCLUSIONS

The inhibitor studied has an excellent inhibition effect for the corrosion of mild steel in 1 M HCl. The high inhibition efficiencies of Palasha (*Butea monosperma*) leaves extract were attributed to the adherent adsorption of the inhibitor molecules on the mild steel surface. Potentiodynamic polarization studies revealed that the studied inhibitor is mixed type inhibitor. The results demonstrate that the inhibition by the Palasha (*Butea monosperma*) leaves extract were attributable to the adsorption of molecules on mild steel surface. On the other hand, values of the obtained double layer capacitance ( $C_{dl}$ ) have shown a tendency to decrease, which can result from a decrease in local dielectric constant and/or an increase in thickness of the electrical double layer. Quantum chemical approach is adequately sufficient to predict the structure and molecule suitability to be an inhibitor.

## References

1. A. Singh, E.E. Ebenso, M.A. Quraishi, *Int. J. Electrochem. Sci.* 7 (2012) 3409.
2. M.A. Quraishi, A. Singh, V.K. Singh, D.K. Yadav, A.K. Singh, *Mater. Chem Phys.* 122(2010) 114.
3. A. Singh, I. Ahamad, V.K. Singh, M.A. Quraishi, *J. Solid State Electr.* 15 (2011) 1087.
4. A. Singh, V.K. Singh, M.A. Quraishi, *Int. J. Corros.* doi:10.1155/2010/275983.
5. A. Singh, V.K. Singh, M.A. Quraishi, *J. Mater. Environ. Sci.* 1(2010) 162.
6. A. Singh, V.K. Singh, M.A. Quraishi, *Rasayan J. Chem.* 3 (2010) 811.
7. A. Singh, I. Ahamad, V.K. Singh, M.A. Quraishi, *Chem. Engg. Comm.* 199(2012) 63.
8. A. Singh, M.A. Quraishi, *Int. J. Corros.* doi:10.1155/2012/897430.
9. A. Singh, M.A. Quraishi, *J.O.C.P.R.* 4 (2012) 322.
10. A. Singh, M.A. Quraishi, *Res. J. Recent. Sci.* 1 (2012) 57.
11. M.A. Quraishi, D.K. Yadav, I. Ahamad, *The Open Corros. J.* 2 (2009) 56.
12. R. Li, Z.T. Jiang, *Flav. Frag. J.* 19 (2004) 311.
13. L. Wang, *Analyt. Chim. Act.* 647 (2009) 72.
14. M.G. Fontana, . *Corrosion Engineering*, Mcgrawhill, Singapore, 1987, 173.
15. A.M. Badiea, K.N. Mohana, *J. Mater. Eng. Perform.* 18(2009) 1264.
16. M.A. Amin, S.S. Abd El-Rehim, E.E.F. El-Sherbini, R.S. Bayyomi, *Electrochim. Act.* 2007, 52, 3588.
17. M. Kedam, O.R. Mattos, H. Takenouti, *J. Electrochem. Soc.* 128 (1981) 257.
18. C.S. Hsu, F. Mansfeld, *Corros.* 57 (2001) 747.
19. M.S. Morad, A.M.K. El-Dean, *Corros. Sci.* 48 (2006) 3398.
20. A. Yurt, A. Balaban, S. Ustun Kandemir, G. Bereket, B. Erk, *Mater. Chem. Phys.* 85(2004) 420.
21. W.H. Li, Q. He, S.T. Zhang, C.L. Pei, B.R. Hou, *J. Appl. Electrochem.* 38 (2008) 289.
22. G. Ji, S.K. Shukla, P. Dwivedi, S. Sundaram, R. Prakash, *Ind. Eng. Chem. Res.* 50 (2011) 11954.

23. Gaussian 03, Revision E.01, Frisch, M.J.; Trucks, G.W.; Schlegel, H.B.; Scuseria, G.E.; Robb, M.A.; Cheeseman, J.R.; Montgomery, Jr. J.A.; Vreven, T.; Kudin, K.N.; Burant, J.C.; Millam, J.M.; Iyengar, S.S.; Tomasi, J.; Barone, V.; Mennucci, B.; Cossi, M.; Scalmani, G.; Rega, N.; Petersson, G.A.; Nakatsuji, H.; Hada, M.; Ehara, M.; Toyota, K.; Fukuda, R.; Hasegawa, J.; Ishida, M.; Nakajima, T.; Honda, Y.; Kitao, O.; Nakai, H.; Klene, M.; Li, X.; Knox, J.E.; Hratchian, H.P.; Cross, J.B.; Bakken, V.; Adamo, C.; Jaramillo, J.; Gomperts, R.; Stratman, R.E.; Yazyev, O.; Austin, A.J.; Cammi, R.; Pomelli, C.; Ochterski, J.W.; Ayala, P.Y.; Morokuma, K.; Voth, G.A.; Salvador, P.; Dannenberg, J.J.; Zakrzewski, V.G.; Dapprich, S.; Daniels, A.D.; Strain, M.C.; Farkas, O.; Malick, D.K.; Rabuck, A.D.; Raghavachari, K.; Foresman, J.B.; Ortiz, J.V.; Cui, Q.; Baboul, A.G.; Clifford, S.; Cioslowski, J.; Stefanov, B.B.; Liu, G.; Liashenko, Piskorz, A. P.; Komaromi, I.; Martin, R.L.; Fox, D.J.; Keith, T.; Al-Laham, M.A.; Peng, C.Y.; Nanayakkara, A.; Challacombe, M.; Gill, P.M.W.; Johnson, B.; Chen, W.; Wong, M.W.; Gonzalez, C.; Pople, J.A.; Gaussian, Inc., Wallingford CT, 2007.
24. I. Ahamad, R. Prasad, M.A. Quraishi, *Corros. Sci.* 52 (2010) 3033.
25. I. Ahamad, R. Prasad, M.A. Quraishi, *J. Solid State Electrochem.* 14 (2010) 2095.
26. D.K. Yadav, M.A. Quraishi, B. Maiti, *Corros. Sci.* 55 (2011) 254.
27. R.S. Goncalves, D.S. Azambuja, A.M. Serpa Lucho, *Corros. Sci.* 44 (2002) 467.
28. G.N. Mu, T.P. Zhao, M. Liu, T. Gu, *Corros.* 52 (1996) 853.